Research Article Adv. Mat. Lett. 2013, **4**(3), 196-201 ADVANCED MATERIALS *Letters*

www.amlett.org, www.amlett.com, DOI: 10.5185/amlett.2012.7390 Published online by the VBRI press in 2013

Low temperature sensing of NO_2 gas using SnO_2-ZnO nanocomposite sensor

Rakesh Kumar Sonker[1], Anjali Sharma[2], Md. Shahabuddin[2], Monika Tomar[3], Vinay Gupta[2*]

[1]*Department of Physics, Bundelkhand University, Jhansi (U.P.), India*
[2]*Department of Physics and Astrophysics, University of Delhi, Delhi, India*
[3]*Department of Physics, Miranda House, University of Delhi, Delhi, India*

[*]Corresponding author. Tel.: (+91) 9811563101, 9555638102; E-mail: drguptavinay@gmail.com

Received: 12 July 2012, Revised: 18 October 2012 and Accepted: 10 November 2012

ABSTRACT

In the present work an effort has been made to synthesize nanocrystalline composites (NCC) of Zinc oxide and Tin oxide (ZSO) using chemical route for efficient sensing of NO_2 gas at lower operating temperature. The structural, microstructural and optical information have been revealed by X-ray diffraction (XRD), Atomic force microscopy (AFM) and UV-Visible spectroscopy respectively. Sensor structure showed a better sensing response ($S \sim 6.64\times10^2$) at a relatively low operating temperature of 70 °C for 20 ppm NO_2 gas with an average response time of about 2 min. The sensing response characteristics for NO_2 gas has been compared with corresponding results obtained for pure SnO_2 and ZnO thin film based sensor structure. Copyright © 2013 VBRI press.

Keywords: SnO_2; nanocomposites; NO_2 gas; thin film.

Rakesh Kumar Sonker was born in Jaunpur (Varanasi), India in August, 1983. Currently, he is pursuing his Ph.D. from Babasaheb Bhimrao Ambedkar University Lucknow. He received his B.Sc. and M.Sc. degree in Physics in the year 2004 and 2008 respectively, from V.B.S. Purvanchal University, Jaunpur (U.P.). He also received Master of Philosophy in Physics (Nanotechnology) in the Year 2011, from Bundelkhand University, Jhansi (U.P.), India.

Anjali Sharma was born in Delhi, India, in June 1985. She received her B.Sc. and M.Sc. degrees in Physics in the year 2006 and 2008 respectively, from University of Delhi. Presently she is a Junior Research Fellow pursuing her Ph.D. program from University of Delhi, Delhi. Her research interests are in gas sensor systems that include sensor characterization and development of metal oxide films for sensor coatings. She is also working towards the fabrication of MEMS based Electronic-Nose for gas sensing applications.

Md Shahabuddin born in 1979 at Nalanda (Bihar), India. He received his M.Sc. and Ph.D. degrees in Physics in 2003 and 2008 from Magadh University and Veer Kunwar Singh University respectively. Presently he is working as a Research Associate with Prof. Vinay Gupta at Department of Physics and Astrophysics, University of Delhi, India. His field of research interest is in the area of condensed matter physics and is focussed on synthesis and characterization of Ceramics. He is currently working towards thin films of metal oxides, polymers and growth of nanostructures for gas sensing applications.

Monika Tomar was born in Delhi, India, in April 1976. She received her B.Sc., M.Sc. and Ph.D. degrees in Physics in 1996, 1998 and 2005 respectively, from the University of Delhi. Presently she is Assistant Professor at Miranda House, University of Delhi, India. Her research interests include piezoelectric thin films for Surface acoustics wave devices and sensors, oxide thin films and nanostructures for gas sensing and biosensing applications, photonic devices etc.

Vinay Gupta was born in Mujjaffar Nagar (U.P), India, in March, 1967. He received his B.Sc., M.Sc., and Ph.D. degrees in physics 1987, 1989 and 1995, respectively from the University of Delhi, India. Subsequently he joined DDU College, University of Delhi as Assistant professor. Presently he is Professor in the Department of Physics and Astrophysics, University of Delhi, India. He is a senior member of IEEE. His current research interests are in piezoelectric, ferroelectric and semiconducting thin films, gas/ bio sensors, Electro-optic applications, oxide nanostructures for multi functional applications etc.

Introduction

Tin oxide has been widely used for various catalytic applications, gas sensing, transparent conducting electrodes and liquid crystal displays, etc. **[1–5]**. As an n-type semiconductor with a wide energy band gap, tin oxide spans a wide range of applications from conductive electrodes and transparent coatings, to heterojunction solar cells, and chemical sensors **[6, 7]**. SnO_2 posses excellent capability of exchange of oxygen from the atmosphere due to natural non- stoichiometry, that makes it the most suitable material for gas sensing application. The adsorption/desorption of oxygen on the surface of SnO_2 is the key parameter for change in conductance. The adsorbed oxygen on the surface (or grain boundaries) of SnO_2 captures the free electrons and becomes O^{-2}. It is important to point out that chemisorption of oxygen is crucial for gas sensing mechanism. Gas sensing properties depend on microstructure, impurities and size effect of crystallites. It is well-known that gas-sensing characteristics of SnO_2 can be dramatically altered by controlling the morphological and microstructural features such as particle size, shape, surface/volume ratio, and porosity. Recently nanostructures are reported to be advantageous for the gas sensing application due to their higher surface/ volume ratio. SnO_2 nanoparticles have been reported to be prepared by using different chemical methods such as precipitation, hydrothermal, sol–gel, gel-combustion and spray pyrolysis **[3–10]**. Among them, sol- gel method has the advantage of low temperature processing and the surface is free from the O–H groups, which affects its properties **[6, 8]**. SnO_2 nanostructures have been found to be promising for gas sensors to detect gases such as NO, NO_2, CO, H_2S, C_2H_5OH etc. **[11-15]** however, the sensors based on SnO_2 nanostructures demand higher operating temperatures. On the other hand, the practical on field gas sensors demand room temperatures operating sensors with enhanced response characteristics for trace level detection of harmful gases. ZnO is another material utilized for the fabrication of gas sensors; however, their sensing response is not so promising though the operating temperatures are low. Hence, a composite structure of SnO_2 with ZnO may be beneficial in reducing the operating temperature with enhanced sensing response. NO_2 is the major cause of formation of ground-level ozone in the stratosphere, acid rains, and an active ingredient to global warming. Exposure to high concentrations of NO_2 can make living organisms more susceptible to bacterial infections and lung cancer. Just like other pollutants, nitrogen dioxide affects people with existing medical conditions more severely than healthy people. The available NO_2 sensors are operative at very high temperature (150–800 ^oC) with low sensing response (2-100) even in higher concentrations as shown in **Table 1 [16-25]**. Efforts are continuing towards the development of NO_2 gas sensors aiming with enhanced response along with reduction in operating temperature by incorporating some catalysts or dopants as shown in **Table 1**. Thus in the present work an effort has been made to develop a SnO_2 nanoparticles doped with ZnO nanoparticles based gas sensor to detect trace level NO_2 gas at lower operating temperature.

Table 1. Literature survey on catalyst modified SnO_2 based NO_2 gas sensors.

Material used	Method	Catalyst / doping	Temp (ºC)	Sensitivity (Concentration)	Response/ Recovery time	Reference
SnO_2 thin film	Slide off transfer printing	WO_3	400	8 (100 ppm)	20 sec / 80 sec	**16**
SnO_2 thick film	Chemical route	Au	300	3.5 (2000 ppb)	20 min/ 50 min	**17**
SnO_2 thin film	Sputtering	Mo	270	20 (10 ppm)	-	**18**
SnO_2 thick film	Screen Printing	WO_3-Au	-	1 (10 ppm)	2 min/ 3 min	**19**
SnO_2 pellet hetrojunction	Powder mixing (Ball milling)	WO_3	300	6.5 (5 ppm)	-	**20**
SnO_2 nanowires	Evaporation	Ru	100	3500 (200 ppm)	100 sec/ 300 sec	**21**
SnO_2 thin film	Wet Chemical	Fe_2O_3	170	110 (1000 ppm)	5 min/ 40 min	**22**
SnO_2 thin film	Sol gel	Indium	150	72 (500 ppm)	2 sec/2 min	**23**
SnO_2 nanofibres	Pulse Laser Depostion	ZnO	180	100 (3.2 ppm)	4 min/ 8 min	**24**
SnO_2 nanowires	Two-Step Vapor Growth	ZnO	300	12.3 (10 ppm)	5 sec/ 12 sec	**25**

Experimental

Materials and methods

Tin (IV) chloride pentahydrate ($SnCl_4.5H_2O$), Isopropanol, propanol, Zinc acetate, Lithium Hydroxide, Ethanol and n-Butyl Acetate used for the sensor preparation were purchased from Sigma Aldrich Chemical Co. with 99.99% purity. A mixture of 12.37 g tin tetrachloride ($SnCl_4.5H_2O$ 99.99%) with 15 g isopropanol was prepared. This is an exothermic reaction, hence the solution was cooled down to room temperature and 3.42 g water in 10 g propanol mixture was added for hydrolysis reaction forming the sol of SnO_2 nanoparticles.

0.01 M of Zinc acetate dihydrate was dissolved in the 75 ml of boiling ethanol (75 ℃) in a round bottom flask fitted with a condenser at atmospheric pressure. The solution is refluxed at 75℃ for about 30 minutes and subsequently allowed to cool at room temperature to give a transparent and stable Zn based precursor. In another beaker, 0.014 M of lithium hydroxide monohydrate was dissolved in 50 ml of ethanol ultrasonically to accelerate the reaction at room temperature. A clear solution is obtained after sonication for about 25-30 min. The hydroxide containing solution was added drop wise to the acetate containing solution at room temperature under vigorous magnetic stirring, and finally a transparent ZnO sol is obtained after hydrolyzing the precursor.

The alcoholic solution of zinc acetate is heated at 75℃ to prepare an intermediate species through hydrolysis and condensation. The acetic acid produced during the heat treatment reacts with ethanol and results in the generation of additional water through an esterification process. The addition of LiOH to the transparent precursor leads to the formation of ZnO nanoparticle sol. The prepared ZnO nanoparticles were added into SnO_2 nanoparticle colloidal solution in the ratio of 60:40 (SnO_2:ZnO). SnO_2 and ZnO:SnO_2 sol were used to deposite respective thin films on corning glass and inter digital electrode (IDEs)

patterned on corning glass substrates by spin coating. The samples were annealed at 500 °C for 1 hour in atmospheric air.

The sensing response characteristics of SnO_2 and $ZnO:SnO_2$ nanocomposite thin films were studied using the films deposited on IDE/glass substrates as shown in **Fig. 1**. The Pt IDEs were patterned over the corning glass substrates using conventional photolithography, prior to deposition of sensing layer ($ZnO:SnO_2$) nanocomposite thin film). The platinum thin film of 90 nm thickness was deposited by RF sputtering using platinum metal target in 100% Ar. In order to improve the adhesion of Pt on corning glass substrate an ultra thin (10 nm) buffer layer of Titanium was sputtered prior to Pt deposition.

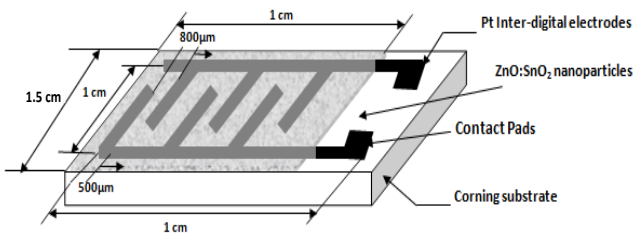

Fig. 1. Schematic of gas sensor structure.

Characterization

Thickness and surface roughness of deposited thin films were measured using a Veeco Dektak 150 surface profiler. Crystalline structure and surface morphology of the sensing layer were studied using Bragg–Brentano (θ–2θ) scan of a X-ray Diffractometer (Bruker D8 Discover) using the CuKα1 source (λ = 0.154 nm) and Atomic force microscopy (Veeco DICP2) respectively. A Double Beam UV–visible Spectrophotometer (Perkin Elmer, Lambda 35) was used to study the optical properties of ZnO and SnO_2 thin films.

Sensing test chamber

NO_2 gas sensing characteristics of sensors were studied in a specially designed "gas sensor test rig (GSTR)" having a glass test chamber. NO_2 gas was introduced into the glass test chamber using calibrated leaks through needle valves. A pirani gauge with a rotary pump was used to control the flow of target gas in the test chamber. Vacuum of the order of ~ 10^{-3} Torr was first created in the test chamber and subsequently a mixture of the known concentration of target gas and clean (dry synthetic) air was introduced till the test chamber acquired the atmospheric pressure to ensure that the target gas was free from any other disturbing gas. The creation of vacuum ensures the removal of any foreign gas molecules from the test chamber. The measurements were carried out in static mode. At the time of recovery of the senor, target gas was flushed out of the test chamber (by creating vacuum again) and the clean dry air was introduced. The sensor was placed on a temperature controlled heating block inside the glass test chamber and spring loaded platinised contacts were used to measure the sensor response as a function of temperature (30–150 °C). At each temperature the sensor was first stabilized in air to obtain a stable resistance value. Target gas (NO_2) of specific concentration was introduced into the test chamber and changes in the sensor resistance were recorded after every second using a data acquisition system consisting of a digital multi-meter (Keithley 2700) interfaced with a computer. The sensor response for an oxidizing gas such as NO_2 is defined as:

$$S = (R_g - R_a)/ R_a$$

where, R_a and R_g are the resistances of the sensor in the presence of atmospheric air and target gas respectively. The response time was measured as the time taken by the sensor to acquire the 90% of its maximum resistance value in the presence of target oxidizing gas. Once the maximum resistance value is attained, the target gas was flushed out of the test chamber and sensor was allowed to regain its initial resistance value in atmospheric air while keeping the sensor at the same temperature. Time taken by the sensor to reacquire about 10% higher value of its initial resistance in the presence of atmospheric air is considered as the recovery time.

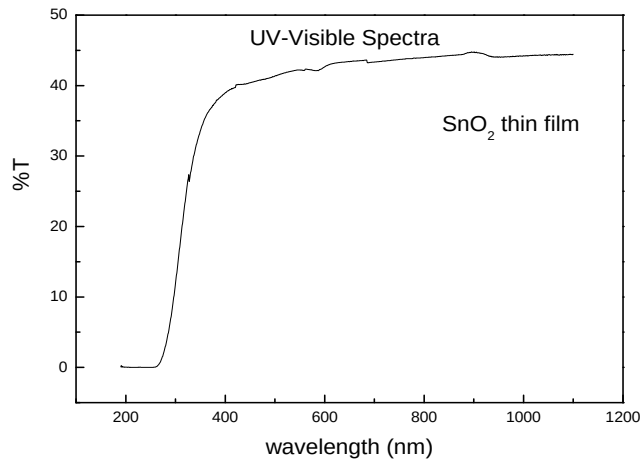

Fig. 2. Transmittance spectra of SnO_2 thin film.

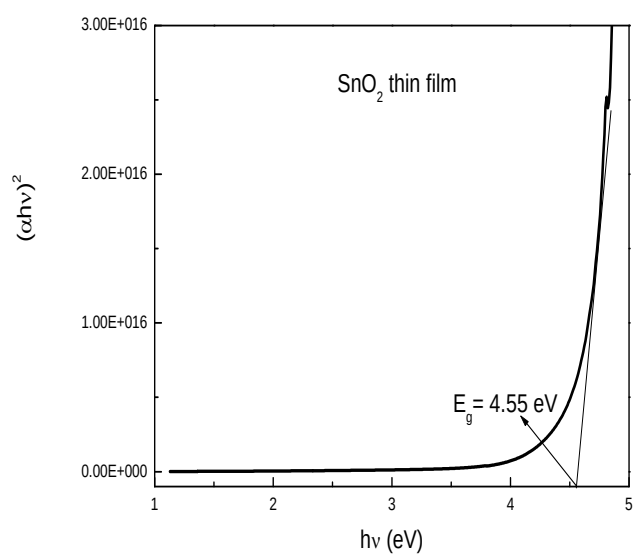

Fig. 3. Tauc plot of $(\alpha h\nu)^2$ versus hν of SnO_2 thin film.

Results and discussion

The optical transmission spectra of the as grown SnO_2 thin films (650 nm thin) deposited separately on corning glass substrate was measured in the wavelength range of 190 to 1100 nm, and the variation is shown in **Fig. 2**. SnO_2 thin film exhibits a high transmission (>40%) in the visible region and show a sharp fundamental absorption edge at around 340 nm.

Optical band gap of the SnO_2 thin film deposited on corning glass substrate, was calculated from the intercept on energy axis obtained by extrapolating the linear portion of the Tauc plot of $(\alpha h\nu)^2$ *vs* photon energy ($h\nu$) as shown in **Fig. 3**. Error in the determination of band gap value was less than 5%. Estimated value of band gap for as-grown SnO_2 thin film is found to be 4.55 eV and is close to the actual values for SnO_2 thin films (4.3 eV) grown by various techniques. Similarly the UV visible spectra of the as deposited ZnO:SnO_2 nanocomposite thin film is shown in **Fig. 4** having high transmission of >80% in the visible region. The value of bandgap (**Fig. 5**) increases slightly for ZnO:SnO_2 composite thin film with the incorporation of ZnO nanoparticles to 4.6 eV.

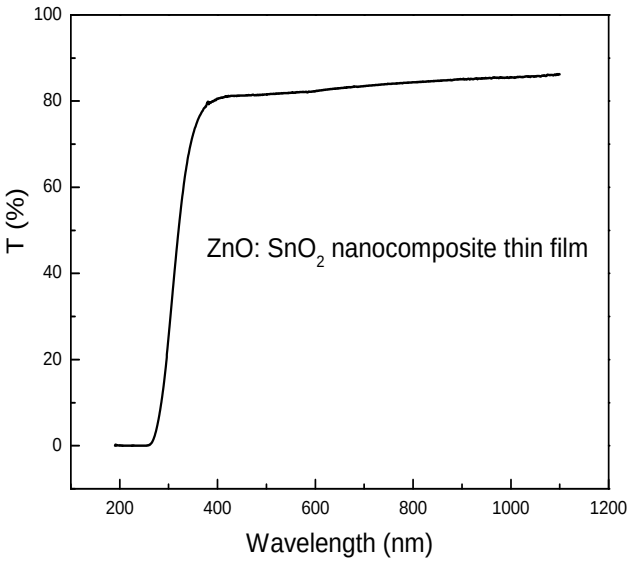

Fig. 4. Transmittance spectra of ZnO:SnO_2 nanocomposite thin film.

The as-grown SnO_2 and ZnO:SnO_2 nanocomposite thin films were found to be amorphous, and become nanocrsytalline after a post deposition annealing treatment at 500 ^oC for 1 h in air. The annealed thin films were found to be smooth, transparent and strongly adherent to the substrate. **Fig. 6** shows the XRD pattern of SnO_2 thin film. Broad and well defined reflections corresponding to (110), (101) and (211) planes of SnO_2 were observed at 26.2^o, 33.8^o and 51.9^o respectively for the deposited SnO_2 film and are in good agreement to the corresponding values reported for rutile structure **[16]**. The values of lattice constants ('a' and 'c') estimated from XRD data for the SnO_2 thin films are found to be 4.62 Å and 3.21 Å respectively. **Fig. 3** shows the XRD pattern obtained for the ZnO:SnO_2 composite thin film. It is observed that at 37.7^o a hump is seen which corresponds to the (101) reflection plane of ZnO **[26, 27]**.

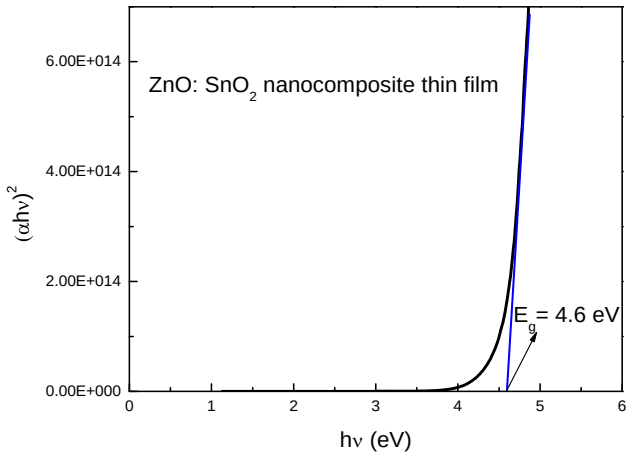

Fig. 5. Tauc plot of $(\alpha h\nu)^2$ versus hν of ZnO:SnO_2 nanocomposite thin film.

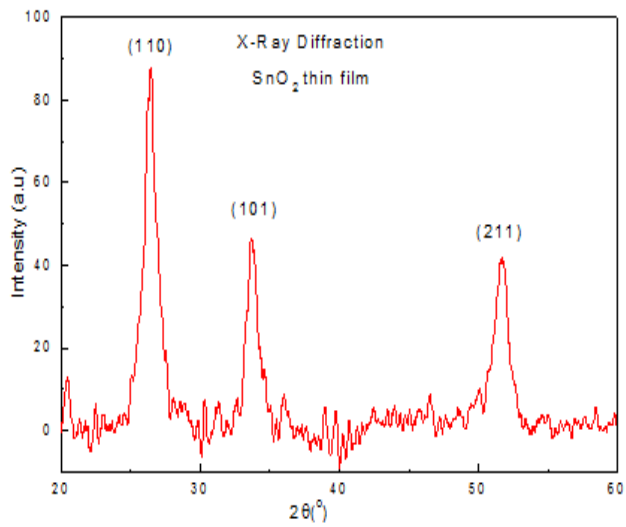

Fig. 6. X-Ray Diffraction of the SnO_2 thin film.

Using the Scherrer's formula the grain size of the deposited SnO_2 and ZnO:SnO_2 nanocomposite thin film was found to be ~9.8. nm and ~8.1 nm respectively which is contributing to higher surface to volume ratio beneficial for gas sensing application. Thus XRD studies shows that the SnO_2 thin film and ZnO: SnO_2 nanocomposite thin films deposited using sol-gel techniques are found to be nanocrystalline in nature.

AFM images of the SnO_2 and ZnO:SnO_2 nanocomposite sensor structures are shown in **Fig. 7.** The results show that the films are nanocrystalline with high surface roughness. Grain size is found to be reduced for the ZnO:SnO_2 nanocomposite thin film sensor structure with high roughness which are known to be important for obtaining enhanced gas sensing response characteristics **[28]**.

Fig. 8 shows the variation in resistance with time for SnO_2 thin film based sensor structure at an operating temperature of 70 ^oC towards 20 ppm NO_2 gas. When target gas (NO_2) was inserted in the chamber, resistance of the film increases because of oxidizing behavior of NO_2 gas. SnO_2 responds to NO_2 gas in the following way **[29].**

$$NO_2 + Sn^{2+} \xrightarrow{adsorption} (Sn^{3+} - NO_2^-) \xrightarrow{desorption} (Sn^{3+} - O^-) + NO$$

$$2(Sn^{3+} - O^-) \xrightarrow{desorption} 2Sn^{2+} + O_2$$

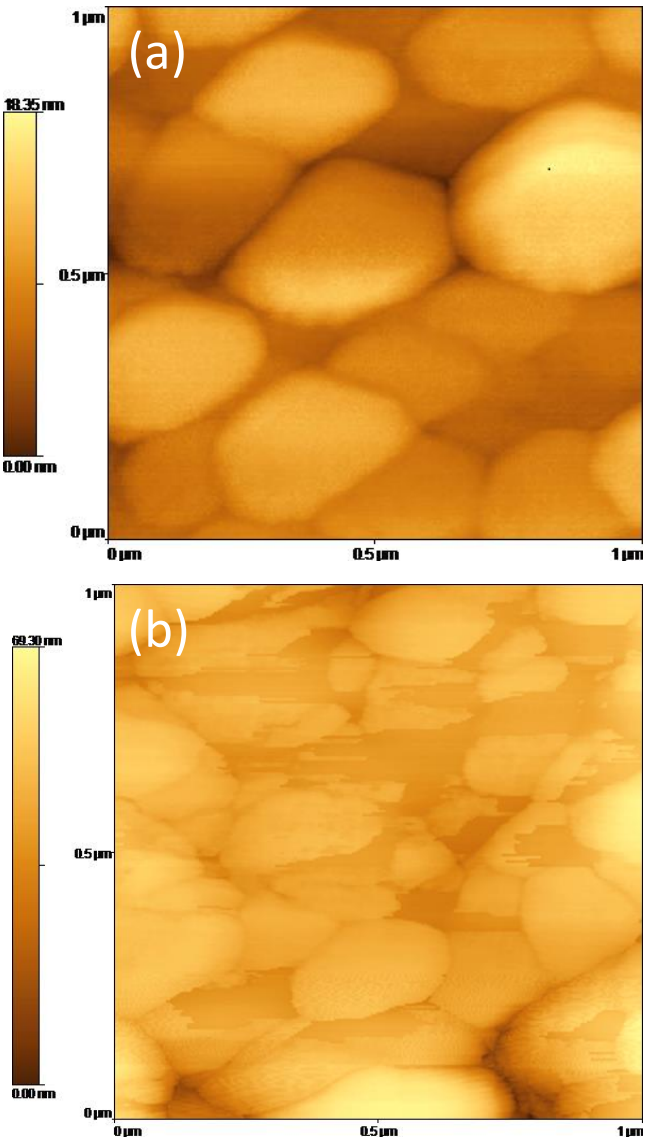

Fig. 7. Atomic force micrograph of (a) SnO_2 thin film (b) ZnO:SnO_2 thin film.

On the SnO_2 surface, NO_2 gas reacts with Sn sites and captures electrons resulting in decrease in conductivity thus increasing the resistance of the film. It can also be observed from **Fig. 8** that the sensor shows a sensor response of 141 with slow response time of ~3 min when the target gas was inserted into the chamber and the sensor resistance recovers back in 7 min after flushing out the gas from the chamber.

Fig. 9 and **10** show the change in sensor resistance with time for the ZnO:SnO_2 nanocomposite sensor structure towards 20 ppm NO_2 gas at an operating temperature of 50 ^oC and 70 ^oC respectively. It can be observed from figures 9 and 10 that with the incorporation of ZnO nanoparticles in SnO_2 nanoparticles colloidal solution, the sensing response has been increased to 621 and 727 at operating temperatures of 50 ^oC and 70 ^oC, respectively.

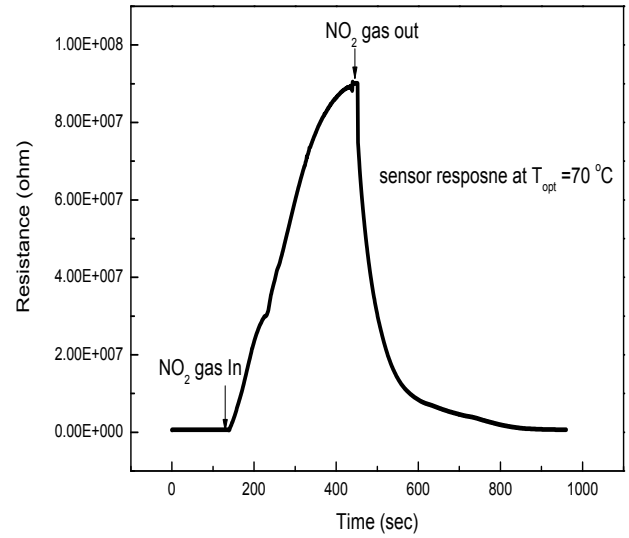

Fig. 8. Variation in resistance with time for SnO_2 thin film towards 20 ppm NO_2 gas.

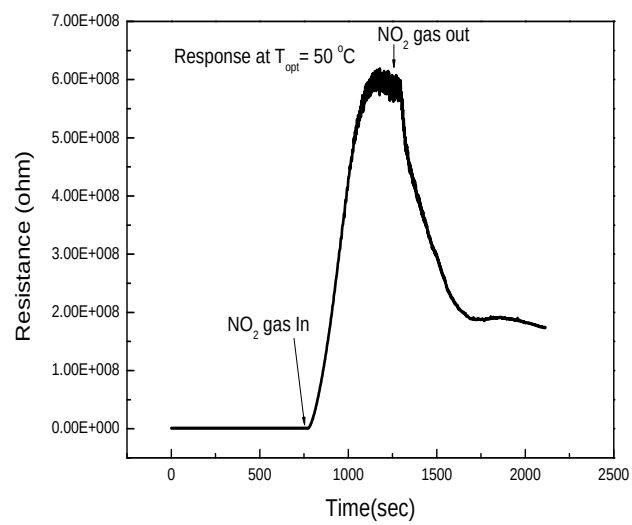

Fig. 9. Variation of resistance with time at 50 ^oC for ZnO: SnO_2 nanocomposite thin film towards 20 ppm NO_2 gas.

It can also be observed that at 50 ^oC the sensor did not recover back to its initial resistance while as at an operating temperature of 70 ^oC the sensor recovers back to its initial resistance. However, the response (t_{res}) and recovery (t_{rec}) times have not shown much improvement. The increased senor response with the incorporation of ZnO may be attributed to the reduction in grain size as observed from AFM images (**Fig. 7**). The reduced grain size provides higher surface to volume ratio allowing more NO_2 gas molecules to react with the sensor surface. When NO_2 gas interacts with ZnO:SnO_2 surface, it interacts with SnO_2 in the same manner as mentioned earlier but when it interacts with ZnO surface it captures electrons from physisorbed oxygen species (O_2^-) and gets desorbed as NO gas molecules even at lower operating temperatures **[30]**.

$NO_{2(gas)} + e^- \rightarrow NO_2^-{}_{(ads)}$

$NO_2^-{}_{(ads)} + O^-{}_{(ads)} + 2e^- \rightarrow NO_{(gas)} + 2O_2^-{}_{(ads)}$

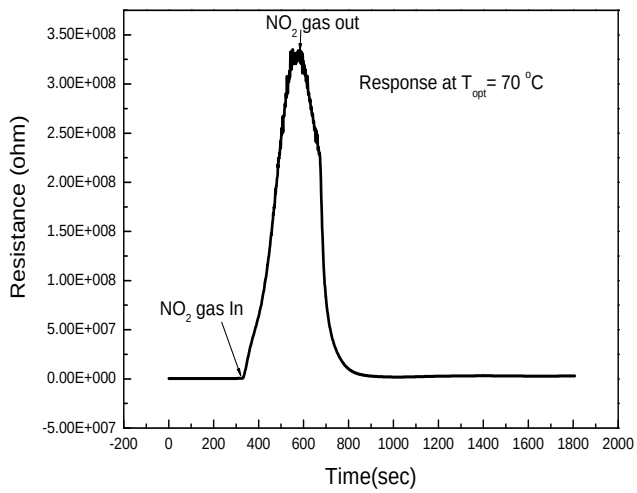

Fig. 10. Variation of resistance with time at 70 °C for ZnO: SnO_2 nanocomposite thin film towards 20 ppm NO_2 gas.

Thus the number of reacting sites increases in the case of ZnO:SnO_2 surface in comparison to pure SnO_2 sensor surface. Thus even at lower operated temperature of 70 °C the sensor response is more in the case of ZnO: SnO_2 sensor (727) as compared to pure SnO_2 sensor (141). The results are promising for the fabrication of low temperature (<100 °C) operating NO_2 gas sensor. Besides the reduced grain size and increased surface roughness, the increased number of reacting sites due to the presence of ZnO in SnO_2 is responsible for the enhanced sensing response at an operating temperature of 70 °C.

Conclusion

SnO_2 thin film and ZnO:SnO_2 nanocomposite thin film based sensor structure have been designed for the trace level (20 ppm) detection of NO_2 gas at low operating temperatures (<100 °C). ZnO:SnO_2 nanocomposite thin film based sensor response of about 727 at a low operating temperature of 70 °C with moderate response and recovery times. Nanoporous surface morphology having nanocrystalline grains are found to be important for obtaining enhanced response characteristics.

Acknowledgements

The authors are thankful to Department of Science and Technology (DST), Department of Information Technology (DIT), NPMASS and University of Delhi for the financial support for carrying out this research work. One of the author (AS) is grateful to the Council of Scientific and Industrial Research (CSIR) for the research scholarship.

Reference

1. Chopra, K.L.; Major, S.; Pandya, D.K., Thin Solid Films **1983**, 102, 1 **DOI**: 10.1016/0040-6090(83)90256-0.
2. Kilic, C.; Zunger, A., Phys. Rev. Lett. **2002**, 88, 095501. **DOI:** 10.1103/PhysRevLett.88.095501
3. Chen, Z.W.; Lai, J.K.L.; Shek, C.H., Phys. Rev. B **2004**, 70, 165314. **DOI:** 10.1103/PhysRevB.70.165314
4. Dieguez, A.; Rodriguez, A.R.; Vila, A.; Morante, J.R., J. Appl. Phys. **2001**, 90, 1550. **DOI**:10.1063/1.1385573
5. Arai, T., J. Phys. Soc. Jpn. **1960**, 15, 916. **DOI:** 10.1143/JPSJ.15.916
6. Zhang, J.; Gao, L.; J. Solid State Chem. **2004,** 177, 1425. **DOI:**10.1016/j.jssc.2003.11.024
7. Fraigi, L.; Lamas, D.G.; de Reca, N.E.W., Nanostruct. Mater. **1993**, 11, 311. **DOI:**10.1016/S0965-9773(99)00046-X
8. Jeong, J.; Choi, S.P.; Chang, C.I.; Shin, D.C.; Park, J.S.; Lee, B.T.; Park, Y.J.; Song , H.J.; Solid State Commun. **2003**, 127, 595. **DOI:** 10.1016/S0038-1098(03)00614-8
9. Santos, L.R.B.; Chartier, T.; Pagnoux, C.; Baumard, J.F.; Santillii, C.V.; Pulcinelli, S.H.; Larbot, A., J. Eur. Ceram. Soc. **2004**, 24, 3713. **DOI:**10.1016/j.jeurceramsoc.2004.03.003
10. Grzeta, B.; Tkalcec, E.; Goebbert, C.; Takeda, M.; Takahashi, M.; Nomura, K.; Jaksic, M., J. Phys. Chem. Solids **2003**, 63, 765. **DOI:** 10.1016/S0022-3697(01)00226-8
11. Chowdhuri, A.; Gupta, V.; Sreenivas, K.; Kumar, R.; Mozumdar, S.; Patanjali, P.K., Appl. Phys. Let, **2004**, 84,1180. **DOI** 10.1063/1.1646760
12. Wang, Y.; Jiang, X.; Xia, Y.; J. Amer. Chem. Soc., **2003,** 125,16176. **DOI:** 10.1021/ja037743f
13. Liu, Y.; Koep, E.; Liu, M.A, Chem. Mat., **2005**, 17, 3997. **DOI:** 10.1021/cm050451o
14. Chen, Y.J.; Nie, L.; Xue, X. Y.; Wang, Y.G; Wang, T.H., Appl. Phys. Let., **2006,** 88, 083105. **DOI:**10.1063/1.2166695
15. Chen, Y.J.; Xue, X.Y.; Wang, Y.G.; Wang, T.H., Appl. Phys. Let., **2005**, 87, 233503. **DOI:**10.1063/1.2140091
16. Hyodo T.; Mori T.; Kawahara A.; Katsuki H.; Shimizu Y.; Egashira M.,Sens & Act B, **2001,** 77, 41. **DOI:** 10.1016/S0925-4005(01)00670-0
17. Abbas M.N.; Moustafa G.A; Gopel W; Analytica Chimica Acta **2001,** 431, 181. **DOI:** 10.1016/S0003-2670(00)01222-8
18. Zampiceni E.; Comini E.; Faglia G.; Sberveglieri G.; Kaciulis S;, Pandolfi L.; Viticoli S.; Sens & Act B **2003**, 89, 225. **DOI:** 10.1016/S0925-4005(02)00469-0
19. Su P.-G.; Jang W.R; Pei N. F.; Talanta **2003,** 59, 667. **DOI:** 10.1016/S0039-9140(02)00582-9
20. Ling Z.; Leach C.; Sens & Act B **2004,** 102, 102. **DOI:** 10.1016/j.snb.2004.02.017
21. 21. Ramgir N.S.; Mulla I. S.; Vijayamohanan K. P.; Sens & Act B **2005**, 107, 708. **DOI:** 10.1016/j.snb.2004.12.073
22. Rumyantseva M.; Kovalenko V.; Gaskov A.; Makshina E.; Yuschenko V.; Ivanova I.; Ponzoni A.; Faglia G.; Comini E.; Sens & Act B **2006**, 118, 208. **DOI:** 10.1016/j.snb.2006.04.024
23. Kaur. J.; Kumar R.; Bhatnagar M.C.; Sens & Act B **2007,** 126, 478. **DOI:** 10.1016/j.snb.2007.03.033
24. Park J.-A.; Moon J.; Lee S.J;, Kim S.H; Chu H.Y; Zyung T.; Sens & Act B **2010,** 145, 592. **DOI:** 10.1016/j.snb.2009.11.023
25. Hwang I.S; Kim S.J.; Choi J.K;, Choi J.; Ji H.; Kim G.T.;, Cao G.; Lee J.H.; Sens & Act B **2010**, 148, 595. **DOI**: 10.1016/j.snb.2010.05.052
26. Sharma P.K; Dutta R.K; Pandey A.C; Adv. Mat. Lett. 2011, 2(4), 246-263; **DOI**: 10.5185/amlett.2011
27. Srivastava R.; Yadav B. C.; Adv. Mat. Lett. **2012**, 3(3), 197-203 **DOI:** 10.5185/amlett.2012.4330
28. Sharma, A.; Tomar, M.; Gupta, V.; Sens. Act. B, **2011**, 156, 743. **DOI:** 10.1016/j.snb.2011.02.033
29. Sharma, A.; Tomar, M.; Gupta, V.; Sens. Act. B, Article in press , **2011** **DOI:** 10.1016/j.snb.2011.10.014
30. Oh E.; Choi H.Y.; Jung S.H;, Cho .S.; Kim J.C; Lee K.H.;, Kang S.W.;, Kim J.; Jeong S.H.; Sens. & Act. B **2009**,141, 239. **DOI:** 10.1016/j.snb.2009.06.03

